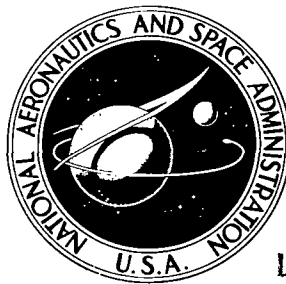


NASA TECHNICAL NOTE



NASA TN D-5331

C. 1

LOAN COPY: RETL
AFWL (WLLI-
KIRTLAND AFB, NM



NASA TN D-5331

DYNAMIC PERFORMANCE ANALYSIS OF
A FUEL-CONTROL VALVE FOR USE
IN AIRBREATHING ENGINE RESEARCH

by Peter G. Batterton and John R. Zeller

Lewis Research Center

Cleveland, Ohio



DYNAMIC PERFORMANCE ANALYSIS OF A FUEL-CONTROL VALVE FOR
USE IN AIRBREATHING ENGINE RESEARCH

By Peter G. Batterton and John R. Zeller

Lewis Research Center
Cleveland, Ohio

NATIONAL AERONAUTICS AND SPACE ADMINISTRATION

For sale by the Clearinghouse for Federal Scientific and Technical Information
Springfield, Virginia 22151 - CFSTI price \$3.00

ABSTRACT

The analysis of a fast-response fuel-control valve for use in turbojet engine research is presented. This analysis includes cases where the valve is (1) closely coupled to the engine spray nozzles and (2) located some distance from the engine, thus requiring connection by a hydraulic transmission line. The analysis results in a complete non-linear model and an equivalent linearized model for both cases. The dynamic performance of the analytical models is presented and compared against corresponding experimental fuel-flow response data. A discussion is included which demonstrates how operating conditions affect fuel-flow frequency response.

DYNAMIC PERFORMANCE ANALYSIS OF A FUEL-CONTROL VALVE FOR USE IN AIRBREATHING ENGINE RESEARCH

by Peter G. Batterton and John R. Zeller

Lewis Research Center

SUMMARY

An analysis of a fast-response fuel-control valve with a reducing pressure regulator is presented. This type of fuel-control valve is often used for dynamic and steady-state engine studies. A nonlinear analytical model for this valve is developed, which accurately predicts the dynamic performance of fuel flow from the valve in response to an input command. Since the fuel-flow response can be uncoupled from the valve actuating servo, this servo is not considered in this report. Many experimental configurations require that the fuel control be located some distance from the engine, thus requiring an interconnecting transmission line. The analysis is extended to include a transmission line between the valve and the load.

A simplified linearized equivalent of the nonlinear analytical model is also derived and found to be an adequate representation for the valve. This linearized equivalent is particularly useful for the prediction of fuel-flow dynamic performance, both bandwidth and damping, for any load configuration. Also, the resulting transfer functions are useful in system performance evaluations. Results are included to demonstrate how this linear analytical model can be used to show some of the effects on the dynamic performance due to various changes in operating parameters.

The transmission line degrades the amplitude frequency response of the fuel system. In addition, the time delay introduces an undesirable phase shift. Both effects can be tolerated for dynamic studies, but they seriously handicap the use of the valve in advanced engine control systems. The use of a transmission line should be avoided whenever possible.

INTRODUCTION

Renewed interest in turbine engine research studies, both steady-state and dynamic,

has created a need for a fast-response, high-performance fuel-control valve. Such a device should be able to (1) accurately control steady-state engine fuel flow and (2) provide controlled dynamic fuel-flow disturbances for the determination of the dynamic characteristics of various engine components. With these capabilities, the fuel-control valve can be employed within a control loop to facilitate the evaluation of new and more sophisticated engine control concepts.

In reference 1, it was concluded that a fuel-control device based on the principle of reducing fuel supply pressure to maintain a constant regulated pressure drop across a variable area orifice best satisfies these requirements. The hydromechanical portion of this device controls output fuel flow in proportion to the area of a fuel metering orifice and independent of output pressure. Metering orifice area is controlled by an electrohydraulic servo actuation system. Fuel-control valve performance can be considered independently of the performance of the fuel valve servo. Thus, this report is restricted to fuel-flow performance with respect to a metering orifice area input.

In order to efficiently use this fuel-control valve for a specific application, it is necessary to understand and predict its dynamic performance for each set of operating conditions. To facilitate this understanding, we will present a detailed analysis of this hydromechanical control device operating directly into an orifice output termination (engine spray nozzles). Actual experimental installations often require the fuel-control device to be located some distance from the spray nozzle load. Therefore, a long line is required to connect the two elements, and the dynamics of this transmission line will be included in the analysis of the fuel-flow high-frequency dynamic performance. This inclusion will supplement the analysis presented in reference 1. To assist in predictions of dynamic performance, we will also derive a simplified linearized analytical model of this fuel-control valve and its connected load.

PHYSICAL DESCRIPTION

Figure 1 shows the general arrangement of a fuel-control valve with a reducing valve pressure regulator. This regulator employs a piston-actuated variable orifice and a preloaded spring that combine to regulate the pressure drop across the control or fuel metering orifice. This pressure drop is held to a value proportional to the force of the preloaded spring. The regulating device is designed to be sensitive enough to maintain this pressure nearly constant over the complete range of flows and output pressure variations. As a result, the control orifice flow is proportional to the control orifice area.

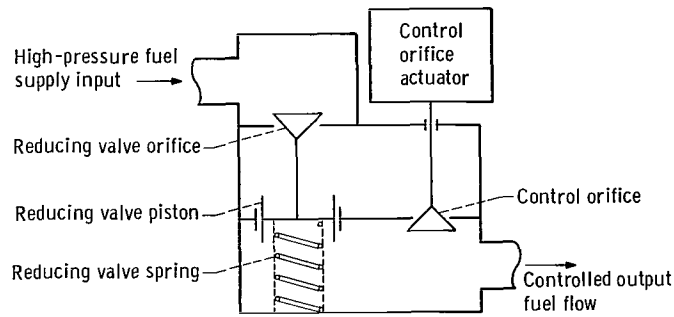


Figure 1. - Fuel-control valve with reducing valve pressure regulator.

ANALYTICAL DESCRIPTION

Figure 2 shows a more detailed version of the hydromechanical portions of the fuel throttling device of figure 1. It also shows the valve output loaded by a fixed orifice with and without the transmission line. This type of load typically represents the spray nozzles of a turbojet engine. In the next sections, a detailed nonlinear analytic representation of this hydromechanical device is derived.

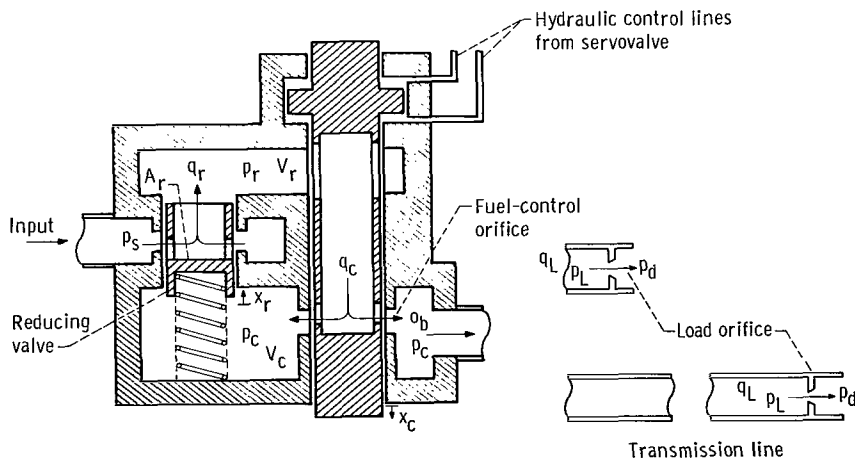


Figure 2. - Cross-sectional view of fuel-control valve.

Orifice Equations

The basic orifice equation (ref. 2) is

$$q = CA \sqrt{\frac{2}{\rho}} \sqrt{\text{Pressure drop}} \quad (1)$$

Thus, for the load orifice, equation (1) becomes

$$q_L = CA_L \sqrt{\frac{2}{\rho}} \sqrt{p_L - p_d} = K_L \sqrt{p_L - p_d} \quad (2)$$

where

$$K_L = CA_L \sqrt{\frac{2}{\rho}} \quad (3)$$

(All symbols are defined in appendix A.) The pressure p_d is the downstream load orifice pressure. It was held constant at atmospheric pressure for the experimental and analytical results presented in this report. In the case of an active engine, it is equal to combustion chamber pressure. Its effect might well be included in any system analysis. It is included in the equations and computer diagrams of this report for the sake of generality. As explained in reference 1, the type of fuel-control valve analyzed in this report displays the desirable feature of being insensitive to low-frequency downstream pressure fluctuations.

The two variable orifices (control and reducing valve) are rectangular in shape and of constant width. Thus, the equations for the flow are as follows:

$$q_c = K_c x_c \sqrt{p_r - p_c} \quad (4)$$

where

$$K_c = Ch_c \sqrt{\frac{2}{\rho}} \quad (5)$$

and

$$q_r = K_r x_r \sqrt{p_s - p_r} \quad (6)$$

where

$$K_r = C h_r \sqrt{\frac{2}{\rho}} \quad (7)$$

Compressibility Equations

There are two volumes in the fuel-control valve: (1) the volume between the pressure reducing orifice and the control orifice and (2) the volume between the control orifice and the valve output.

If the fuel is considered to be a compressible fluid, the dynamic relation between pressure and volumetric flow through a control volume is as follows (ref. 2):

$$\frac{\dot{p}}{\beta} = \frac{q_{\text{vol, in}} - q_{\text{vol, out}}}{V} \quad (8)$$

For the control volume between the reducing valve orifice and the control orifice:

$$q_{\text{vol, in}} - q_{\text{vol, out}} = q_r - q_c + A_r \dot{x}_r \quad (9)$$

and

$$V = V_r - A_r x_r \quad (10)$$

The third term on the right side of equation (9) is the fuel flow generated by the reducing valve piston motion. Substituting equations (9) and (10) into equation (8) yields

$$\frac{\dot{p}_r}{\beta} = \frac{q_r - q_c + A_r \dot{x}_r}{V_r - A_r x_r} \quad (11)$$

If, for all x_r , $V_r \gg A_r x_r$, then equation (11) reduces to

$$\frac{\dot{p}_r}{\beta} = \frac{q_r - q_c + A_r \dot{x}_r}{V_r} \quad (12)$$

For the control volume between the control orifice and the output

$$q_{\text{vol, in}} - q_{\text{vol, out}} = q_c - q_o - A_r \dot{x}_r \quad (13)$$

and

$$V = V_c + A_r x_r \quad (14)$$

Substituting equations (13) and (14) into equation (8) yields

$$\frac{\dot{p}_c}{\beta} = \frac{q_c - q_o - A_r \dot{x}_r}{V_c} \quad (15)$$

for $V_c \gg A_r x_r$.

Force-Balance Equations

Fuel pressure actuates the reducing valve piston. Therefore, a force-balance equation describes the motion of this spring mass system. For the valve being evaluated in this report, the area of both faces of the reducing valve piston are equal. The equation is

$$M_r \ddot{x}_r + B_r \dot{x}_r + k_r x_r = A_r (p_c - p_r) + F \quad (16)$$

where B_r is a friction force or a force due to velocity. Its value could not be measured and was chosen to give a damping of 0.2 for the left half of equation (16).

Lossless Transmission Line

In a typical test installation, the fuel-control valve may be located some distance from the engine load. If this is the case, then some type of fuel line will connect the valve to this spray nozzle load. For the purposes of this report, this is assumed to be a lossless hydraulic transmission line.

In reference 3 two equations that relate the flows and pressures for the line are of use in this study. These are, in the time domain

$$p_L(t) = p_c(t - \sigma) + Z [-q_L(t) + q_o(t - \sigma)] \quad (17)$$

$$q_o(t) = q_L(t - \sigma) + \frac{1}{Z} [p_c(t) - p_L(t - \sigma)] \quad (18)$$

Nonlinear Block Diagram

The nonlinear block diagram (fig. 3, p. 11) represents symbolically the function of equations (2), (4), (6), (12), and (15) to (18). The inputs to the block diagram are p_d , p_s , F , and x_c .

LINEARIZED FUEL VALVE REPRESENTATION

In actual usage for a dynamics research program, the fuel-control valve is used to modulate fuel flow dynamically about some steady-state operating level of fuel flow. Thus, valve operation will involve small deviations about a selected operating point. This type of operation makes linearized analysis of the describing nonlinear equations an ideal method for evaluating the valve small-disturbance performance. Appendix B includes the linearization of the basic valve equations. Since most experimental modulating signals will be sinusoidal in nature, the linearized equations have been converted to the Laplace domain. Also, from experimental observation and from the nonlinear simulation, the pressure-reducing valve closely regulates the control orifice pressure difference ($p_r - p_c$) to frequencies much higher than those of interest herein. This feature simplifies the resulting linearized equations. The equations resulting from these manipulations and the preceding observations are stated as follows:

$$\Delta Q_c = K_1 \Delta X_c \quad (19)$$

$$\left\{ \left[\frac{A_r(V_r + V_c)}{K_3\beta} \right] S^2 + \left(\frac{V_c}{\beta} + \frac{A_r K_4}{K_3} \right) S \right\} \Delta P_c = \Delta Q_c - \left(1 + \frac{A_r}{K_3} S \right) \Delta Q_o \quad (20)$$

$$\Delta Q_L = K_5 \Delta P_L \quad (21)$$

where

$$K_1 = K_c \sqrt{p_r - p_c} \Big|_{t=T} \quad (22)$$

$$K_3 = K_r \sqrt{p_s - p_r} \Big|_{t=T} \quad (23)$$

$$K_4 = \frac{K_r x_r}{2 \sqrt{p_s - p_r}} \Big|_{t=T} \quad (24)$$

$$K_5 = \frac{K_L}{2 \sqrt{p_L}} \Big|_{t=T} \quad (25)$$

Equation (20) defines the output characteristic of the fuel-control valve. This equation can be used to determine the transfer functions of this device when operating with any load whose input flow ΔQ_O is linearly related to the valve output pressure ΔP_C .

Closed Coupled Load

If the load orifice is connected directly to the fuel-control valve outlet, then $\Delta P_L = \Delta P_C$ and $\Delta Q_O = \Delta Q_L$. Substituting equation (21) into (20), the following transfer function is obtained:

$$\frac{\Delta Q_L}{\Delta Q_C} = \frac{1}{\left[\frac{A_r(V_r + V_c)}{K_3 K_5 \beta} \right] S^2 + \left[\frac{V_c}{K_5 \beta} + \frac{A_r(K_4 + K_5)}{K_3 K_5} \right] S + 1} \quad (26)$$

Equation (26) is in the general form of a second-order transfer function with the natural frequency and damping defined as follows:

(1) For the natural frequency

$$\omega_n = \sqrt{\frac{K_3 K_5 \beta}{A_r(V_r + V_c)}} \quad (27)$$

(2) For the damping coefficient

$$\delta = \frac{1}{2} \left[\frac{V_c}{\beta} + \frac{A_r(K_4 + K_5)}{K_3} \right] \sqrt{\frac{K_3 \beta}{K_5 A_r(V_r + V_c)}} \quad (28)$$

Transmission Line Coupled Load

Equations (17) and (18), which describe the long fuel transmission line, can be linearized directly and result in

$$\Delta p_L(t) = \Delta p_c(t - \sigma) + Z [-\Delta q_L(t) + \Delta q_o(t - \sigma)] \quad (29)$$

$$\Delta q_o(t) = \Delta q_L(t - \sigma) + \frac{1}{Z} [\Delta p_c(t) - \Delta p_L(t - \sigma)] \quad (30)$$

Application of the Laplace transform converts equations (29) and (30) into

$$\Delta P_L = \Delta P_c e^{-S\sigma} + Z (-\Delta Q_L + \Delta Q_o e^{-S\sigma}) \quad (31)$$

$$\Delta Q_o = \Delta Q_L e^{-S\sigma} + \frac{1}{Z} (\Delta P_c - \Delta P_L e^{-S\sigma}) \quad (32)$$

When the long fuel transmission line is used to connect the valve to the load orifice, ΔP_c is no longer equal to ΔP_L and ΔQ_o is no longer equal to ΔQ_L . Therefore, equations (20), (21), (31), and (32) can be combined by standard algebraic means and result in the following transfer function:

$$\frac{\Delta Q_L}{\Delta Q_c} = \frac{2K_5}{\left(1 + \frac{A_r}{K_3} S\right) \left[K_5 (e^{-S\sigma} + e^{S\sigma}) + \frac{1}{Z} (e^{S\sigma} - e^{-S\sigma}) \right] + \left\{ \left[\frac{A_r (K_r + V_c)}{K_3 \beta} \right] S^2 + \left(\frac{V_c}{\beta} + \frac{A_r K_4}{K_3} \right) S \right\} \left[Z K_5 (e^{S\sigma} - e^{-S\sigma}) + e^{-S\sigma} + e^{S\sigma} \right]} \quad (33)$$

If $s = j\omega$, equation (33) becomes

$$\frac{\Delta Q_L}{\Delta Q_c} = \frac{1}{j \left\{ \omega K_6 \cos \omega\sigma + \left[\frac{1}{Z K_5} - \frac{\omega^2 A_r (V_r + V_c) Z}{K_3 \beta} \right] \sin \omega\sigma \right\} + \left\{ \left[1 - \frac{\omega^2 A_r (V_r + V_c)}{K_5 K_3 \beta} \right] \cos \omega\sigma - \omega K_7 \sin \omega\sigma \right\}} \quad (34)$$

where

$$K_6 = \left[\frac{V_c}{\beta} + \frac{A_r (K_4 + K_5)}{K_3} \right] \frac{1}{K_5} \quad (35)$$

and

$$K_7 = \left[\frac{V_c}{\beta} + \frac{A_r \left(K_4 + \frac{1}{K_5 Z^2} \right)}{K_3} \right] Z \quad (36)$$

When $Z = K_5^{-1}$, the load impedance is matched to the transmission line impedance, and the amplitude frequency response of the fuel system will show no degradation due to line resonances. However, matching the line impedance to the load will not reduce the dead time caused by the transmission line. A FORTRAN IV program for computing the frequency response of equation (34) appears in appendix C.

COMPARISON OF DYNAMIC PERFORMANCE, LOAD CLOSE COUPLED

Simulated Nonlinear Model Performance

The nonlinear block diagram of figure 3 was simulated on an analog computer using the parameter values of table I. Figure 4 shows the fuel-flow frequency response for this model with a close coupled load to a small control orifice area input signal. The magnitude of this input signal corresponds to 5 percent, peak-to-peak, of maximum fuel flow, where maximum fuel flow is 38.5 cubic inches per second (630.9 cm³/sec).

Experimental Performance

Figure 5 is a photograph of the experimental valve, disassembled to show the arrangement of its internal parts. The actual frequency response data for this configuration is shown in figure 6. The nonlinear analytical results of figure 4 have been overlaid for comparison purposes. There is close correlation for all values of fuel flow. Experimental fuel flow was determined by measuring the pressure drop across the load orifice.

Linearized Model Performance

For an input of 5 percent, peak-to-peak, of maximum fuel flow, the frequency responses of the linear and nonlinear models are found to be identical. Therefore, the

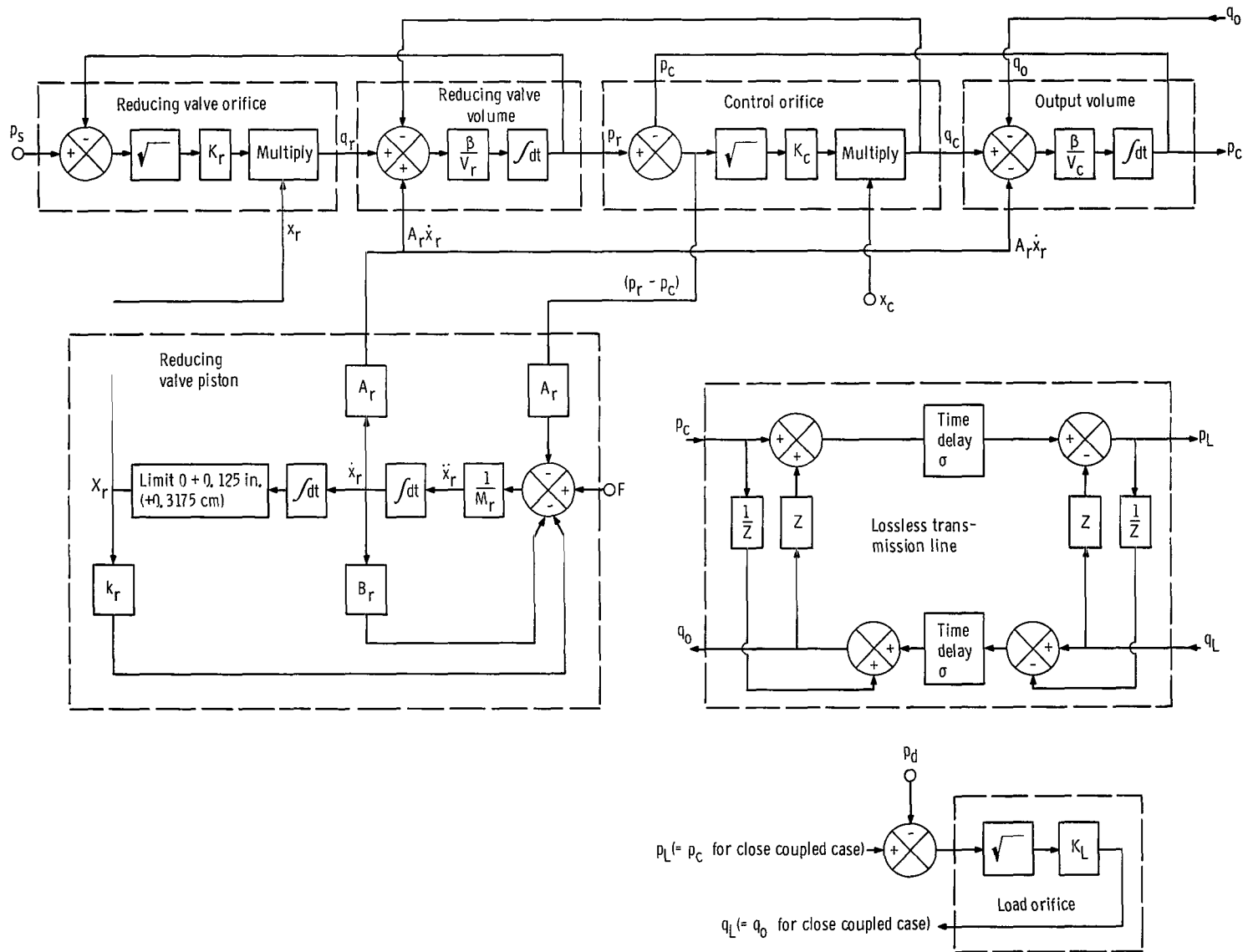


Figure 3. - Nonlinear block diagram of fuel-control valve.

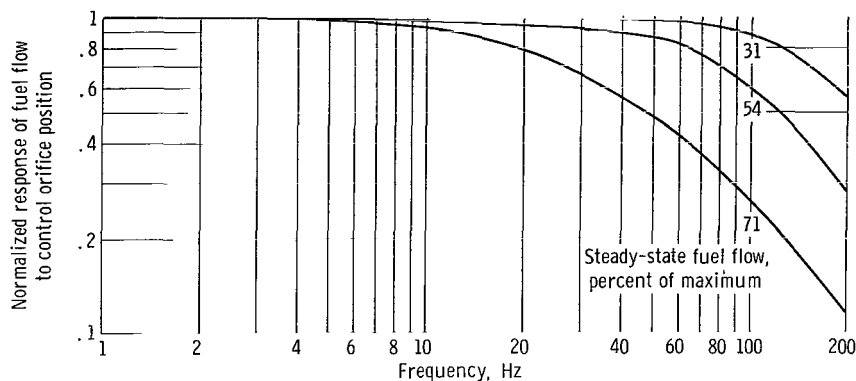


Figure 4. - Fuel-flow frequency response from simulated nonlinear model. Close coupled load.

TABLE I. - FUEL CONTROL VALVE MECHANICAL CONSTANTS

Reducing valve piston area, in. ² ; cm ²	1.0; 6.45
Reducing valve friction, B, (lbf)(sec)/in.; (N)(sec)/cm	0.0633; 0.1109
Reducing valve spring bias, F, lbf; N	140; 623
Control orifice constant, K _c , in. ³ /(sec)(lbf ^{1/2}); cm ³ /(sec)(N ^{1/2})	16.25; 126.26
Load orifice constant, K _L , in. ⁴ /(sec)(lbf ^{1/2}); cm ⁴ /(sec)(N ^{1/2})	1.397; 27.57
Reducing valve orifice constant, K _r , in. ³ /(sec)(lbf ^{1/2}); cm ³ /(sec)(N ^{1/2})	70.4; 547.0
Reducing valve spring constant, k _r , lbf/in.; N/cm	100; 175
Reducing valve piston mass, M _r , (lbf)(sec ²)/in.; (N)(sec ²)/cm	2.51×10 ⁻⁴ ; 4.40
Fuel supply pressure, p _s , psi; N/cm ²	650; 448
Control orifice volume, V _c , in. ³ ; cm ³	7.5; 122.9
Reducing valve volume, V _r , in. ³ ; cm ³	5.55; 90.95
Hydraulic line surge impedance, Z, (lbf)(sec)/in. ⁵ ; (N)(sec)/cm ⁵	9.235; 16.18
Fuel bulk modulus, β, psi; N/cm ²	1.5×10 ⁵ ; 1.04×10 ⁵
Fuel mass density, ρ, (lbf)(sec ²)/in. ⁴ ; (N)(sec ²)/cm ⁴	7.5×10 ⁻⁵ ; 8.02×10 ⁻⁶
Hydraulic time delay, σ, sec	2.6×10 ⁻³
Hydraulic line area, a, in. ² ; cm ²	0.36317; 2.343
Hydraulic line length, l, in.; cm	120; 305

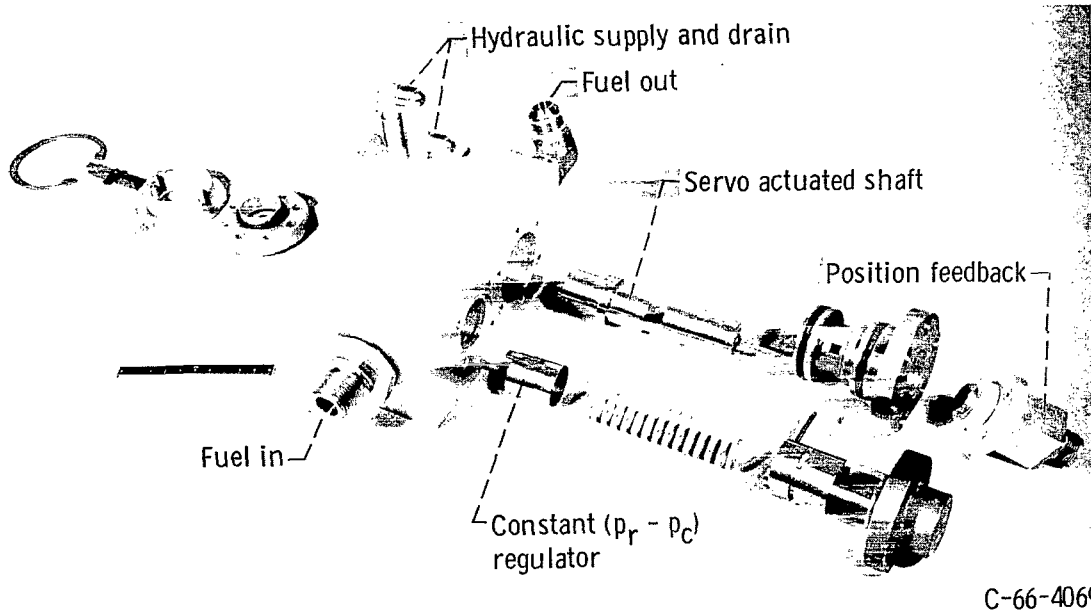


Figure 5. - Research fuel control valve.

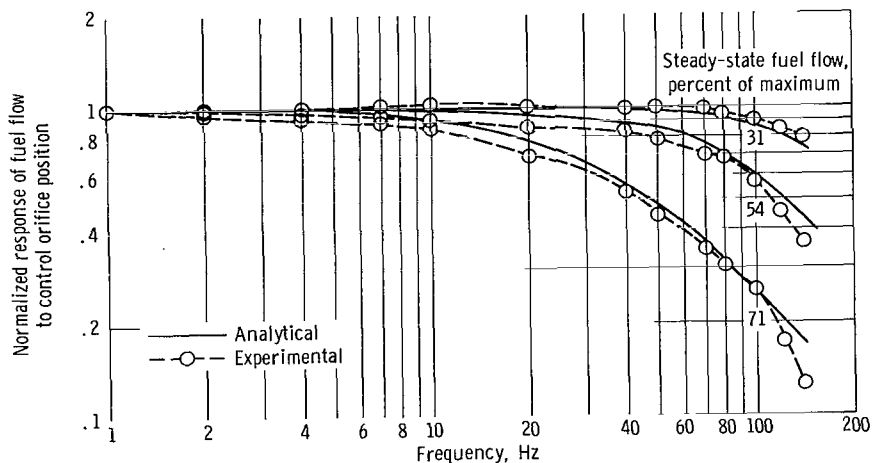


Figure 6. - Comparison of experimental and analytical fuel-flow frequency response. Close coupled load.

linear model is quite adequate for dynamic performance evaluations at these relatively low levels. It should be noted that the valve natural frequency and damping (eqs. (27) and (28)) are dependent on several fixed valve parameters as well as several linearization constants. The linearization constants vary with the steady-state operating point. This variation is evident in the frequency response curves of figures 4 and 6 and in equation (26) for different levels of steady-state fuel flow. It should be noted that dynamic performance or bandwidth degrade as the steady-state fuel flow operating point increases. These three steady-state conditions are tabulated in table II.

TABLE II. - FUEL CONTROL VALVE OPERATING CONDITIONS

[Maximum fuel flow, 38.5 in.³/sec (10.0 gal/min or 630.9 cm³/sec);
fuel supply pressure, 650 psi (448 N/cm²).]

Percent maximum flow	Reducing valve pressure, P_R		Control orifice pressure, P_C		Control orifice length, x_C		Reducing valve length, x_R	
	psi	N/cm ²	psi	N/cm ²	in.	mm	in.	mm
	31	213	147	73	50	63×10^{-3}	1.57	8.13×10^{-3}
54	362	250	222	153	109	2.77	17.38	.441
71	523	361	383	264	144	3.66	34.15	.867

DYNAMIC PERFORMANCE WITH A LONG LINE

Performance of Simulated Model

The nonlinear block diagram of figure 3 was simulated on an analog computer using the parametric values of table I. The 2.6-millisecond time delay was simulated with a fourth-order Pade approximation (ref. 4). Dynamic performance was evaluated for the case of a 10-foot (3.048-m) long, 0.75-inch (1.905-cm) outside diameter, stainless-steel fuel transmission line at 54-percent maximum steady-state fuel flow using the same load orifice as the close coupled case. The performance for this condition is given in figure 7. The performance of the close coupled nonlinear model at 54-percent maximum fuel flow is overlayed for demonstration purposes. The effect of the transmission line is considerable, degrading the system bandwidth by nearly a 4 to 1 margin.

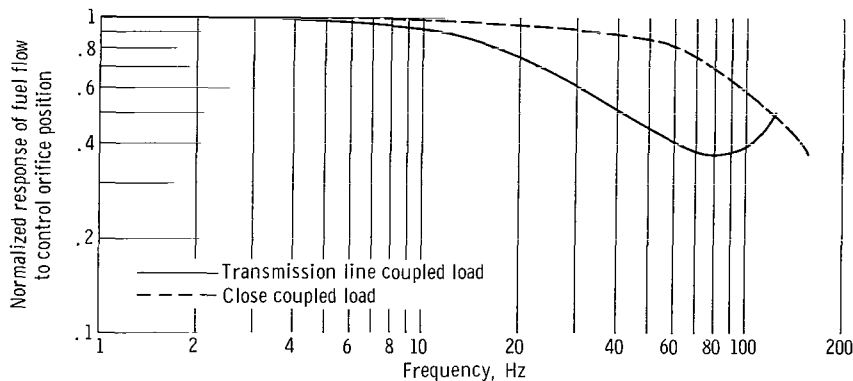


Figure 7. - Comparison of nonlinear model fuel-flow frequency responses for close coupled and transmission line coupled load. Steady-state fuel flow, 54 percent maximum.

Experimental Performance

The experimental frequency response curve obtained at 54-percent maximum flow condition is shown in the curve of figure 8. The analytical performance of figure 7 as obtained from the simulated nonlinear model, has been overlaid for comparison purposes. These results were obtained with a 10-foot (3.048-m) long, 0.75-inch (1.905-cm) outside diameter line. The theoretical effect of line resistance in this particular case was checked (ref. 5) and found to make the model results fall closer to the experimental data. However, the improvement was not significant enough to require the modification of the basic flow equations (17) and (18). In installations in which smaller diameters or longer

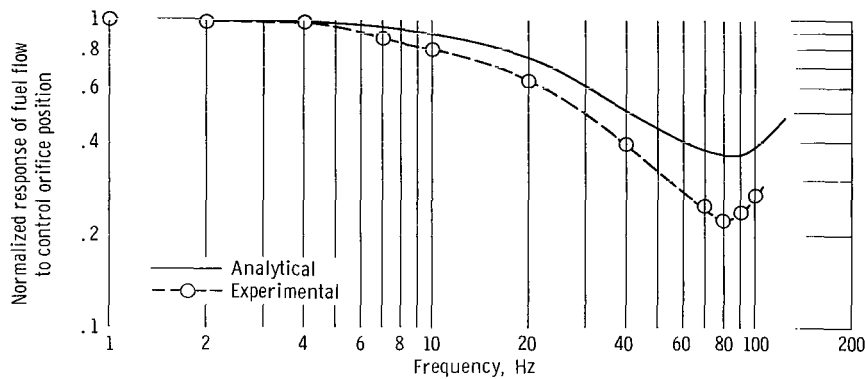


Figure 8. - Comparison of experimental and analytical fuel-flow frequency response. Steady-state fuel flow, 54 percent maximum; transmission line coupled load.

lengths of transmission are used, the effect of this theoretical line resistance may not be negligible.

It should be noted that the attenuation of the analytical model performance is not as great as that of the actual experimental performance. The curves do, however, possess the same "valley" frequency or frequency at which attenuation is a maximum. No explanation for the discrepancy is available. The model, however, should be adequate to approximately predict the degradation that will occur at various frequencies due to the addition of the long transmission line.

Long Line Linear Model

Figure 9 gives the frequency responses for the three conditions of fuel flow as tabulated in table II. The performance of the linear model is again identical to the nonlinear model performance.

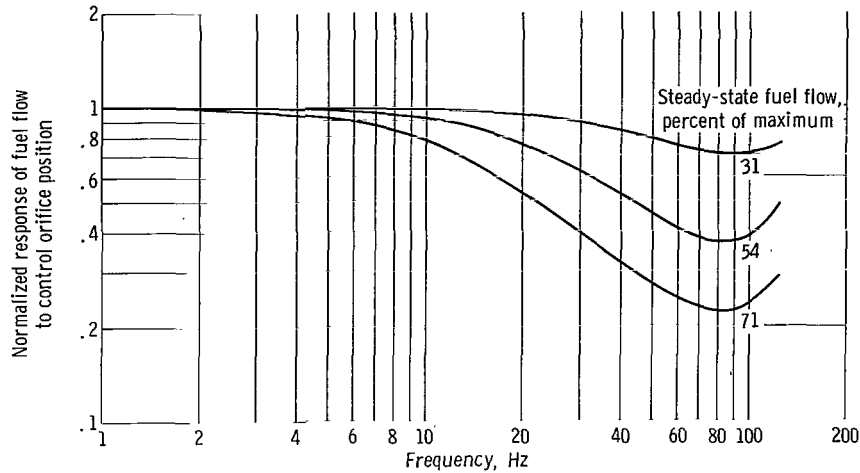


Figure 9. - Frequency response of linear model at different fuel flows. Transmission line coupled load.

Figure 9 shows how the fuel-flow frequency response varies at the three levels of steady-state fuel flow. As mentioned earlier, when the line impedance is equal to K_5^{-1} , the fuel-flow amplitude frequency response shows no degradation due to the transmission line. When the product ZK_5 is less than 1, a valley will occur in the fuel-flow amplitude frequency response at a frequency somewhat less than $1/4\sigma$ hertz, and, when ZK_5 is greater than 1, a peak will occur. Thus, the product ZK_5 could be used as a measure of the line to load matching

$$ZK_5 = \frac{\sqrt{\rho\beta}}{a} \frac{K_L}{2\sqrt{p_L}} = \frac{\rho c K_L^2}{2aq_L} \quad (37)$$

For a given steady-state flow condition, equation (37) shows that the impedance match is proportional to the square of the load orifice constant (thus, the square of the orifice area) and inversely proportional to the transmission line cross-sectional area. Equation (37) also shows that, if the steady-state fuel flow is changed, the impedance match is changed. Thus, if the line impedance is matched to the load for one level of fuel flow, the line and load will not be matched at other levels of fuel flow. For the experimental system described in table I, equation (37) is less than one for all three levels of fuel flow.

DISCUSSION OF DYNAMIC PERFORMANCE AND RECOMMENDATIONS

From the response curves of figure 5, it may be concluded that the nonlinear analytical model is a very good representation of the fuel system with close coupled load. The

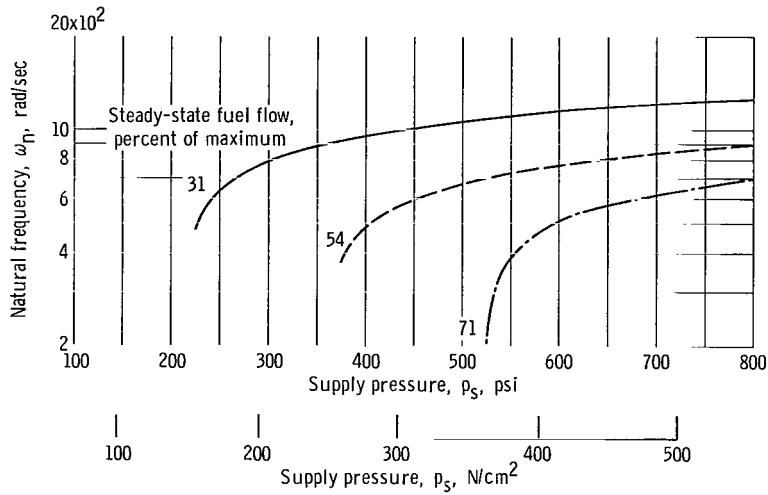


Figure 10. - Effect of supply pressure on valve natural frequency. Load orifice constant at 1.397 inch⁴ per second per pound^{1/2} (27.54 cm⁴/(sec)(N^{1/2})).

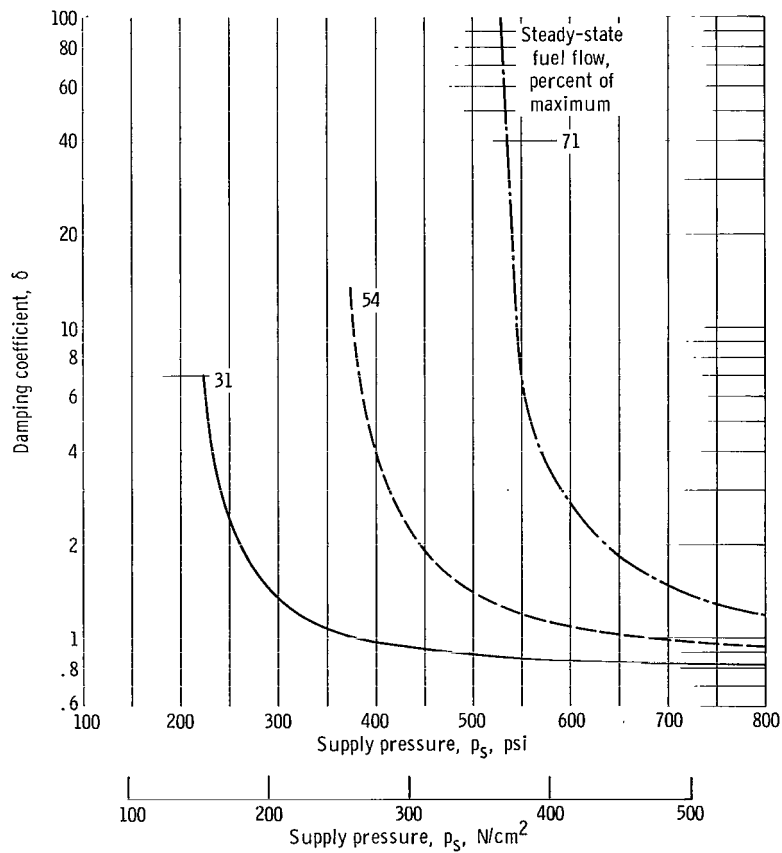


Figure 11. - Effect of supply pressure on valve damping. Load orifice constant at 1.397 inch⁴ per second per pound^{1/2} (27.57 cm⁴/(sec)(N^{1/2})).

second-order linear transfer function describing this configuration also accurately represents the dynamic system. The main advantage of the transfer function linearization is that the fuel system flow response for various conditions can be predicted almost by inspection.

For example, different supply pressures and/or different load orifices may be used. Both parameters affect the values of ω_n and δ , the natural frequency and damping of the valve. Figures 10 and 11 show how ω_n and δ vary, respectively, as functions of the supply pressure with a specific load orifice constant. The value of K_L is 1.397 inch^4 per second per pound^{1/2} ($27.5 \text{ cm}^4/(\text{sec})(\text{N}^{1/2})$). We can see that, as the supply pressure is decreased, ω_n decreases and damping increases. Both effects will degrade the dynamic performance capabilities of the fuel valve. Thus, to operate unattenuated to the highest frequencies, supply pressure should be maintained at the higher level (650 to 800 psi (450 to 550 N/cm^2)).

Figures 12 and 13 show how ω_n and δ vary, respectively, as functions of the load orifice constant K_L with supply pressure held constant. The value of p_s is 650 psi (448 N/cm^2). The natural frequency decreases as the load orifice constant decreases (load orifice area decreasing). However, for the three flows considered, the damping remains nearly constant (between 0.8 and 1.2) over a fairly wide range of load orifices (1.65 to 3.8 $\text{in.}^4/(\text{sec})(\text{lb}^{1/2})$ or 32 to 74 $\text{cm}^4/(\text{sec})(\text{N}^{1/2})$).

The long line linear model is also considered to be sufficiently accurate for determining fuel system flow response with a lossless transmission line coupling the load. The transmission line degrades the amplitude response of the fuel system flow (fig. 7) as well

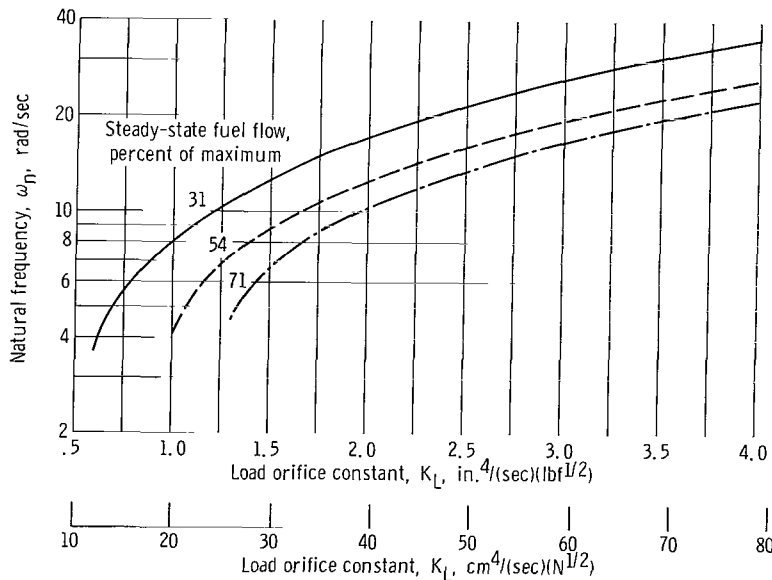


Figure 12. - Effect of load orifice constant on valve natural frequency. Supply pressure constant at 650 psi (448 N/cm^2).

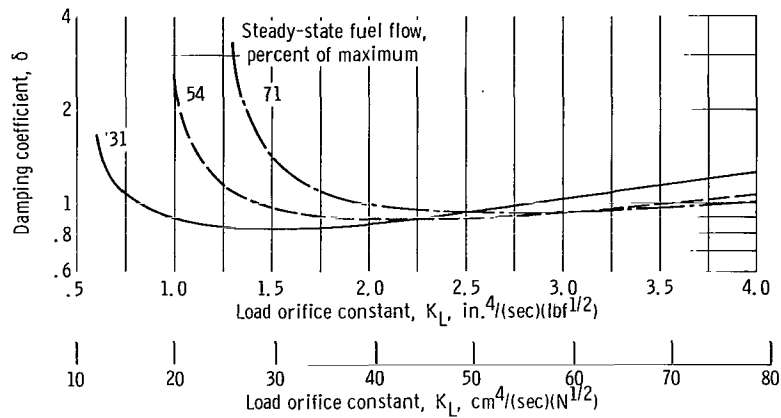


Figure 13. - Effect of load orifice constant on valve damping. Supply pressure constant at 650 psi (448 N/cm²).

as adding phase shift due to its time delay. It is recommended that the use of a transmission line be avoided so that the user can take full advantage of the flow response capabilities of the fuel-control valve. If the transmission line must be used, the analytical models developed in this report can be used to approximately predict the effect of the transmission line on the system flow response.

CONCLUDING REMARKS

An analysis of the fuel-control valve with a pressure reducing regulator, including the effects of a long hydraulic transmission line has been presented. Nonlinear and linear dynamic models of the valve were developed for both the close coupled load and the load coupled by a long hydraulic transmission line. These models predict the performance of these systems up to 100 hertz. Therefore, these models can be used successfully to predict fuel-flow dynamic performance for different configurations and various steady-state operating points.

Lewis Research Center,
 National Aeronautics and Space Administration,
 Cleveland, Ohio, April 26, 1969,
 720-03-00-69-22.

APPENDIX A

SYMBOLS

A	area, in. ² ; cm ²
a	hydraulic transmission line cross-sectional area, in. ² ; cm ²
B	sliding friction, lb-sec/in.; (N)(sec)/cm
C	orifice discharge coefficient
c	velocity of sound in A-1 jet fuel, $\sqrt{\beta/\rho}$, in./sec; cm/sec
F	spring bias force, lb; N
h	orifice width, in.; cm
j	$\sqrt{-1}$, $j^2 = -1$
K	with alphabetic subscripts, orifice constant; with numeric subscripts, linearization constant
k	reducing valve spring constant, lb/in.; N/cm
l	length of hydraulic transmission line, in.; cm
M	mass of piston, (lb)(sec ²)/in.; (N)(sec ²)/cm
ΔP	Laplace transform of Δp , psi; N/cm ²
p	gage pressure, time domain, psi; N/cm ²
ΔQ	Laplace transform of Δq , in. ³ /sec; cm ³ /sec
q	volumetric flow, time domain, in. ³ /sec; cm ³ /sec
S	Laplace transform operator, sec ⁻¹
T	time at which steady-state values exist
t	time, sec
V	volume downstream of variable orifice, in. ³ ; cm ³
ΔX	Laplace transform of Δx , in.; cm
x	variable orifice length, time domain, in.; cm
Z	hydraulic transmission line surge impedance, $\sqrt{\rho\beta/a}$, (lb)(sec)/in. ⁵ ; (N)(sec)/cm ⁵
β	bulk modulus of A-1 jet fuel, psi; N/cm ²
δ	second-order transfer function damping coefficient
θ	phase angle, deg

ρ mass density of A-1 jet fuel, $(\text{lb})(\text{sec}^2)/\text{in.}^4$; $(\text{N})(\text{sec}^2)/\text{cm}^4$
 σ hydraulic transmission line time delay, l/c , sec
 ω frequency, rad/sec

Subscripts:

c control
d drain
L load
n second order transfer function natural frequency
o fuel valve outlet
r reducing valve
s supply
vol, in volume in
vol, out volume out
1-7 linearization

APPENDIX B

LINEARIZATION OF FUEL VALVE EQUATIONS

Repeated are the nonlinear differential equations for the case of the fuel control valve and load orifice.

$$q_c = K_c x_c \sqrt{p_r - p_c} \quad (4)$$

$$q_r = K_r x_r \sqrt{p_s - p_r} \quad (6)$$

$$q_L = K_L \sqrt{p_L} \quad (2a)$$

$$\frac{\dot{p}_r}{\beta} = \frac{q_r - q_c + A_r \dot{x}_r}{V_r} \quad (11)$$

$$\frac{\dot{p}_c}{\beta} = \frac{q_c - q_o - A_r \dot{x}_r}{V_c} \quad (15)$$

$$M_r \ddot{x}_r + B_r \dot{x}_r + k_r x_r = A_r (p_c - p_r) + F \quad (16)$$

From experimental observation and from the nonlinear simulation, the pressure reducing valve closely regulates $p_r - p_c$ to frequencies much higher than those of interest here. Thus, equation (16) becomes

$$0 = A_r (p_c - p_r) + F \quad (B1)$$

Applying the Laplace transform, equation (B1) becomes

$$\Delta P_c = \Delta P_r \quad (B2)$$

Equation (4) is linearized as follows:

$$\Delta q_c = K_1 \Delta x_c + K_2 \Delta p_r - K_2 \Delta p_c \quad (B3)$$

where

$$K_1 = K_c \sqrt{p_r - p_c} \Big|_{t=T} \quad (22)$$

and

$$K_2 = \frac{1}{2} K_c x_c \frac{1}{\sqrt{p_r - p_c}} \Big|_{t=T} \quad (B4)$$

Applying the Laplace transform and substituting equation (B2) yields for equation (B3)

$$\Delta Q_c = K_1 \Delta X_c \quad (19)$$

In the same manner, equations (6) and (2a) are linearized as follows:

$$\Delta q_r = K_3 \Delta x_r - K_4 \Delta p_r \quad (B5)$$

where

$$K_3 = K_r \sqrt{p_s - p_r} \Big|_{t=T} \quad (23)$$

and

$$K_4 = \frac{1}{2} K_r x_r \frac{1}{\sqrt{p_s - p_r}} \Big|_{t=T} \quad (24)$$

$$\Delta q_L = K_5 \Delta p_L \quad (B6)$$

where

$$K_5 = \frac{1}{2} K_L \frac{1}{\sqrt{p_L}} \Big|_{t=T} \quad (25)$$

Applying the Laplace transform yields for equations (B5) and (B6)

$$\Delta Q_r = K_3 \Delta X_r - K_4 \Delta P_c \quad (B7)$$

where

$$\Delta P_r = \Delta P_c \quad (B8)$$

and

$$\Delta Q_L = K_5 \Delta P_L \quad (21)$$

Similarly, equations (11) and (15) yield

$$\Delta P_c S \frac{V_r}{\beta} = \Delta Q_r - \Delta Q_c + S A_r \Delta X_r \quad (B9)$$

where

$$\Delta P_r = \Delta P_c$$

$$\Delta P_c S \frac{V_c}{\beta} = \Delta Q_c - \Delta Q_o - S A_r \Delta X_r \quad (B10)$$

By standard algebraic methods, equations (B7), (B9), and (B10) can be reduced to yield the following equation:

$$\left\{ \left[\frac{A_r (V_r + V_c)}{K_3 \beta} \right] S^2 + \left(\frac{V_c}{\beta} + \frac{A_r K_4}{K_3} \right) S \right\} \Delta P_c = \Delta Q_c - \left(1 + \frac{A_r}{K_3} S \right) \Delta Q_o \quad (20)$$

Equation (20) defines the output characteristic of the fuel-control valve. This equation can be used to determine the transfer function of this device when operating with any load whose input flow ΔQ_o is linearly related to the valve outlet pressure ΔP_c .

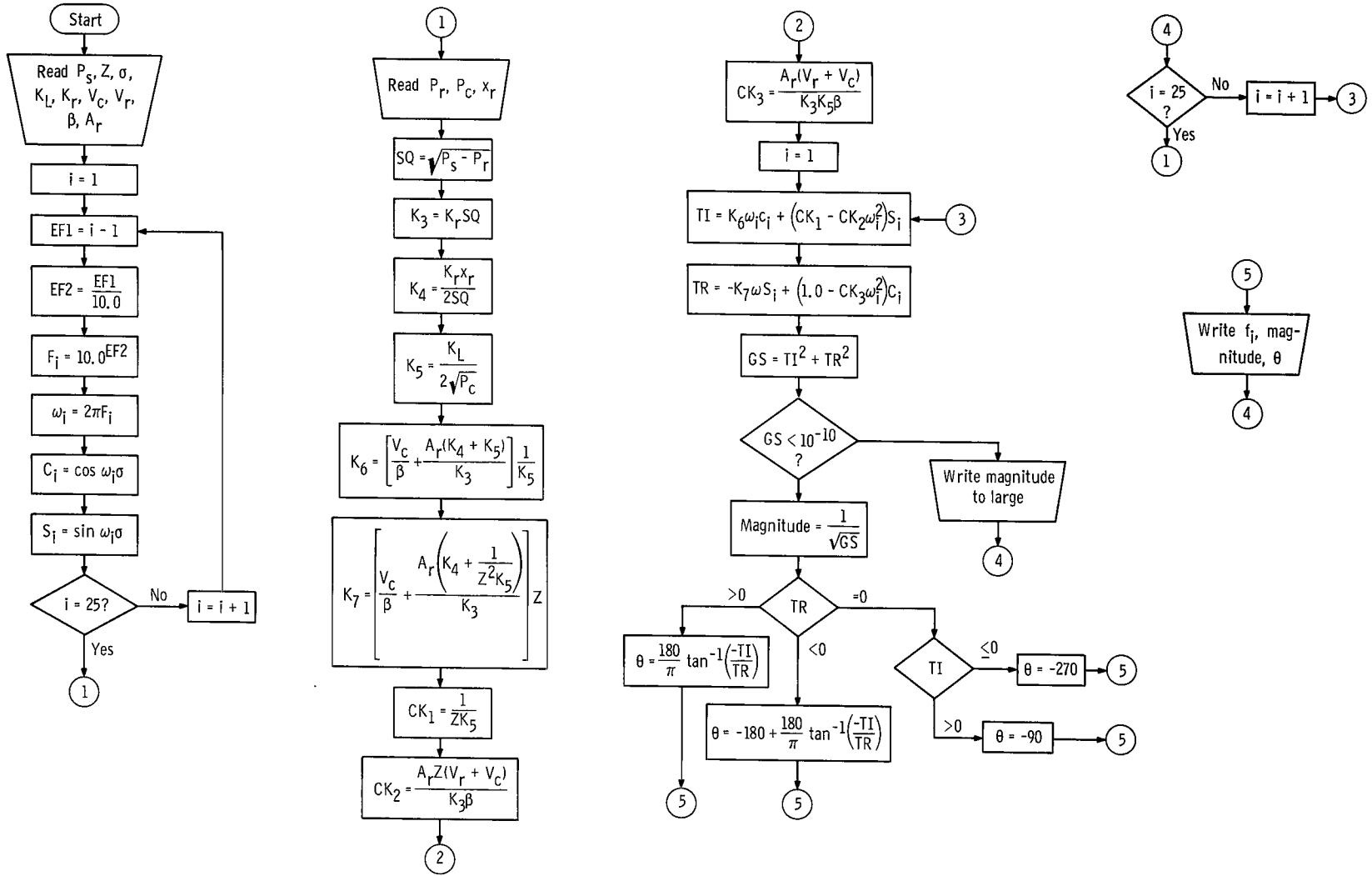
APPENDIX C

DIGITAL COMPUTER PROGRAM AND FLOW DIAGRAM

```

DIMENSION F(25),W(25),C(25),S(25)
READ(5,2) PS,Z,TE,AKL,AKR,VC,VR,B,AR
WRITE(6,2) PS,Z,TE,AKL,AKR,VC,VR,B,AR
DJ 1 I=1,25
EF1=I-1
EF2=EF1/10.0
F(I)=10.0**EF2
W(I)=6.283185*F(I)
C(I)=COS(W(I)*TE)
1 S(I)=SIN(W(I)*TE)
3 READ(5,2) PR,PL,XR
SQ=SQRT(PS-PR)
AK3=AKR*SQ
AK4=0.5*AKR*XR/SQ
AK5=0.5*AKL/SQRT(PL)
AK6=(VC/3+AR*(AK4+AK5)/AK3)/AK5
AK7=(VC/B+AR*(AK4+1.0/(AK5*Z*Z))/AK3)*Z
CK1=1.0/(Z*AK5)
CK2=AR*(VR+VC)*Z/(AK3*B)
CK3=AR*(VR+VC)/(AK3*AK5*B)
WRITE(6,4)
DJ 5 I=1,25
TI=AK6*W(I)*C(I)+(CK1-CK2*W(I)*W(I))*S(I)
TR=-AK7*W(I)*S(I)+(1.0-CK3*W(I)*W(I))*C(I)
GS=TI*TI+TR*TR
IF(GS.LT.1.0E-10) GO TO 10
AMAG=SQRT(1.0/GS)
IF(TR)7,8,9
7 PHASE=-180.0+57.29577*ATAN(-TI/TR)
GJ TO 6
8 IF(TI) 11,11,12
11 PHASE=-270.0
GJ TO 6
12 PHASE=-90.0
GO TO 6
9 PHASE=57.29577*ATAN(-TI/TR)
6 WRITE(6,13)F(I),AMAG,PHASE
GJ TO 5
10 WRITE(6,14)
5 CONTINUE
GJ TO 3
2 FORMAT(3E20.8)
4 FORMAT(1H1,10X,9HFREQUENCY,11X,9HMAGNITUDE,11X,5HPHASE//)
13 FORMAT(1X,1P3E20.8)
14 FORMAT(1X,12HMAG TOO LARGE)
END

```



REFERENCES

1. Otto, Edward W.; Gold, Harold; and Hiller, Kirby W.: Design and Performance of Throttle-Type Fuel Controls for Engine Dynamic Studies. NACA TN 3445, 1955.
2. Stenning, A. H.; and Shearer, J. L.: Fundamentals of Fluid Flow. Fluid Power Control. John F. Blackburn, Gerhard Reethof, and J. Lowen Shearer, eds., Technology Press of M. I. T. and John Wiley & Sons, Inc., 1960, ch. 3, sec. 3.3.
3. Ezekiel, F. D.; and Paynter, H. M.: Fluid-Power Transmission. Fluid Power Control. John F. Blackburn, Gerhard Reethof, and J. Lowen Shearer, eds., Technology Press of M. I. T. and John Wiley & Sons, Inc., 1960, ch. 5, sec. 5.3.
4. Carlson, Alan; Hannauer, George; Carey, Thomas; and Holsberg, Peter J., eds.: Handbook of Analog Computation. Second ed., Electronics Associates, Inc., 1965.
5. Karam, J. T., Jr.: A New Model for Fluidics Transmission Lines. Control Eng., vol. 13, no. 12, Dec. 1966, pp. 59-63.